

## Comparison of Diagnostic Performance Metrics for Test Point Selection in Analog Circuits

Koutaro Hachiya

Faculty of Modern Life  
Teikyo Heisei University  
Tokyo, Japan  
k.hachiya@thu.ac.jp

Atsushi Kurokawa

Graduate School of Science and Technology  
Hirosaki University  
Hirosaki, Japan  
kurokawa@eit.hirosaki-u.ac.jp

**Abstract—** Finding good measurement points in the circuit under test is one of the key issues to increase fault coverage of the structural test. In this paper, diagnostic performance metrics proposed in literature for finding measurement points in analog circuits are compared in terms of four properties. Two of the four properties are confirmed by the experiments using different two normal distribution functions, one for defect-free and another with a defect. According to the comparison result, the guideline for metrics selection is proposed. As a case study, the metrics are applied to finding measurement points to detect open defects of through silicon vias in power distribution networks of 3D-ICs.

### I. INTRODUCTION

Test methods for LSIs (Large-Scale Integrated Circuits) are categorized into the following two approaches.

- *Functional test* checks whether functional specifications are fulfilled – i.e. Black-box test.
- *Structural test* detects defects of each component in circuits under test – i.e. White-box test.

Structural tests offer higher test coverage than functional tests in general, and are hired for testing digital circuits. But for analog circuits, structural test methods have not been matured yet, functional tests are great majority. In typical automotive LSIs, test escapes in analog circuits are of the order of 1 ppm (parts per million) and are at least 10 times more than those in digital circuits [1]. To overcome this situation, structural test of analog circuits has been studied while most of manufacturing tests of analog circuits still hire functional tests in practice. Test item selection procedure in structural tests of catastrophic faults considering process variation is as follows in general [2, 3, 4].

Structural test methods proposed for analog circuits are based on *simulation before test* approach and their typical procedure is as follows [2]. 1) Define *defect models* for all components (active devices, passive devices and wires, etc.) in the circuit under test. 2) Generate a *defect list* which contains all the defects of all the components. 3) Pick up one of the defects from the list and run its fault simulations to calculate effects of

the defect on results of predefined test items. The *fault simulations* generate netlists with the selected defective component and with test vectors and measurements for all test item candidates. To take process variation into account, the simulations also include Monte Carlo analyses with statistical models for the components in the circuit, and measured results have statistical distributions. 4) Evaluate diagnostic performance of each test item to detect the selected defect by using two distributions of its measured result, one with the defect and another without it (i.e. defect-free). 5) Choose the best test item out of the candidates which have the best diagnostic performance to detect the selected defect. 6) Repeat steps 3 to 5 for each defect in the defect list. 7) Determine threshold value for each test item chosen in Step 5 and derive test coverage and yield loss.

To evaluate diagnostic performance of each test item to detect a selected defect in Step4 above, different metrics are proposed in literature [2, 3, 4, 5]. But they have not been compared yet, and we are not sure which one of the metrics to use. In this paper, four diagnostic performance metrics are compared. Using different combinations of two normal distributions, these metrics are calculated and their properties are confirmed by the calculated values. As a case study, the metrics are applied to detecting open-defects of TSVs (Through Silicon Vias) in PDNs (Power Distribution Networks) in 3D-ICs (Three Dimensional Integrated Circuits).

The rest of the paper is organized as follows. In section II, diagnostic performance metrics are reviewed. In section III, the metrics are compared and guideline for selection of the metrics is proposed. In section IV, the metrics are applied to finding measurement points to detect an open defect of TSV in PDN of a 3D-IC, and the simulation results are presented. Section V summarizes conclusions.

### II. DIAGNOSTIC PERFORMANCE METRICS FOR TEST POINT SELECTION

#### A. ROC (Receiver Operating Characteristic) curve

ROC curve visualizes performance of binary classifiers [6]. Binary classifiers classify a given set of instances into two groups. Examples of such classifiers include clinical tests which decide whether positive (abnormal) or negative (nor-

	Defective	Defect-free
Reject	True rejection (TR)	False rejection (FR)
Accept	False acceptance (FA)	True acceptance (TA)

Fig. 1. Confusion matrix.

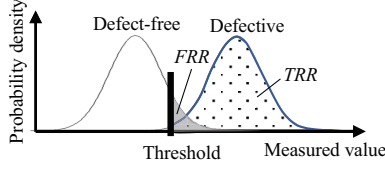


Fig. 2. Probability distributions of measured values for defect-free and defective cases.

mal), and shipment tests at factories which decide whether pass (accept) or fail (reject). ROC curve is extensively used to evaluate performance of medical diagnoses [7, 8], and is proposed to use as a performance metric to select test points in analog circuits [5].

In the context of manufacturing tests, test results fall into one of the four cases in Fig. 1. The case when a defective product is diagnosed as reject is called *true rejection*, and the case when it is diagnosed as accept is called *false acceptance*. The case when defect-free product is diagnosed as accept is called *true acceptance*, and the case when it is diagnosed as reject is called *false rejection*. Hereafter, number of products in each four cases are expressed by  $TR$ ,  $FA$ ,  $TA$  and  $FR$ , then the total number of defective products  $D = TR + FA$  and the total number of defect-free products  $DF = FR + TA$ . Using these numbers, the following four test metrics are defined:

$$\text{True rejection rate } TRR = TR/D \quad (1)$$

$$\text{False acceptance rate } FAR = FA/D \quad (2)$$

$$\text{True acceptance rate } TAR = TA/DF \quad (3)$$

$$\text{False rejection rate } FRR = FR/DF \quad (4)$$

Here we assume that each test item measures a value (e.g. voltage or current, etc.) of each product and diagnoses as *reject* when the value exceeds a pre-defined threshold. The measured values vary from product to product due to variabilities in manufacturing, voltage, temperature and measurement. Therefore, the probability distribution of the measured values for defect-free products and that for defective products look like those depicted in Fig. 2.

ROC curves are two-dimensional graphs in which  $FRR$  is plotted on the  $x$ -axis and  $TRR$  is plotted on the  $y$ -axis as shown in Fig. 3 while changing the threshold in Fig. 2 from  $+\infty$  to  $-\infty$ . The curve depicts relative tradeoffs between benefits (true rejects) and costs (false rejects). When the two probability distributions of defect-free and defective cases are apart enough from each other, the ROC curve looks like the solid line (1) in Fig. 3 and goes up close to  $y$ -axis and then turn right near the

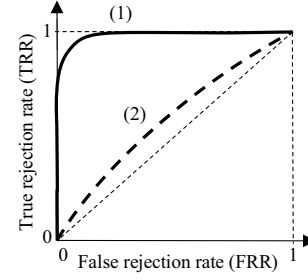


Fig. 3. ROC curves.

point (0,1). When the two distributions are close to each other, the ROC curve looks like the dashed line (2) in Fig. 3 and goes upper right near the straight line connecting the points (0,0) and (1,1). To express diagnostic performance as a single quantity, AUC (Area Under the Curve) is used in general.  $AUC=1$  is the most ideal case.  $AUC=0.5$  is equivalent to random diagnoses. The closer to 1 AUC is, the better its diagnostic performance is. AUC of the curve (1) is larger than that of the curve (2) in Fig. 3 and hence the binary classifier with the curve (1) has better diagnostic performance than that with the curve (2). AUC equals to the probability that a randomly chosen defective product has higher measured value than that of a randomly chosen defect-free product [9].

### B. False Acceptance Rate (FAR)

Ref. [2] proposed to use Bayes risk which is the expected value of costs paid for false rejections and false acceptances as a diagnostic performance metric. We have to know all the probabilities of occurrence of defects to derive the Bayes risk, but that is not practical. Instead of Bayes risk, FAR (False Acceptance Rate) when threshold is set to  $\mu_1 + 3\sigma_1$  is used as a diagnostic performance metric in the experiments conducted in [2], where  $\mu_1$  and  $\sigma_1$  are mean and standard deviation of the probability distribution of measured values in defect-free case. Here the probability distributions of measured values are assumed to be normal distributions. We denote the simplified Bayes risk by  $FAR(w)$  and is defined as

$$FAR(w) = \text{normdist}(\mu_1 + w\sigma_1, \mu_2, \sigma_2), \quad (5)$$

where  $\mu_2$  and  $\sigma_2$  are mean and standard deviation of the probability distribution of measured values in defective case, and  $\text{normdist}(x, \mu, \sigma)$  is the cumulative distribution function of the normal distribution with mean  $\mu$  and standard deviation  $\sigma$  evaluated at the value  $x$ .  $FAR(w)$  is the shaded area shown in Fig. 4.

### C. Normalized Fault Isolation Probability

Ref. [3] proposed *normalized fault isolation probability*  $P_{FI}$  as a diagnostic performance metric which is defined as follows:

$$P_{FI}(w) = \{\text{normdist}(V_{\min}, \mu_1, \sigma_1) + (1 - \text{normdist}(V_{\max}, \mu_2, \sigma_2))\}/2, \quad (6)$$

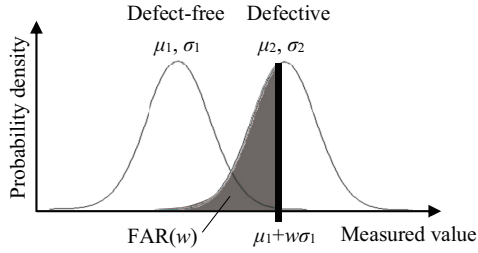


Fig. 4. False Acceptance Rate (FAR).

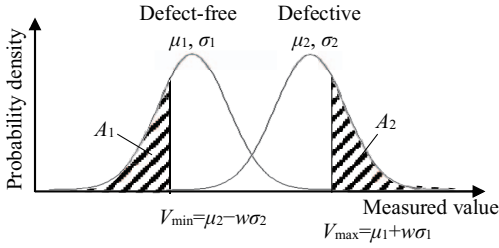


Fig. 5. Normalized fault isolation probability.

where  $V_{\min} = \mu_2 - w\sigma_2$  and  $V_{\max} = \mu_1 + w\sigma_1$ , and  $w$  is an arbitrary positive value.  $P_{FI}(w)$  is a half of the sum of the shaded two areas  $A_1$  and  $A_2$  in Fig. 5. Division by 2 normalizes the sum of the areas.

#### D. Similarity Coefficient

Ref. [4] utilizes normalized cross-correlation of given two waveforms which is a measure of similarity of the two waveforms to evaluate diagnostic performance. The two probability distributions of measured values in defect-free and defective cases are treated as two waveforms  $f(x)$  and  $g(x)$ . Similarity coefficient  $C_s$  of the waveforms is defined as follows.

$$C_s = 1 - \frac{\int f(x)g(x)dx}{\sqrt{\int f^2(x)dx} \sqrt{\int g^2(x)dx}} \quad (7)$$

Its range is from 0 to 1. When  $f(x) = g(x)$ ,  $C_s = 0$ . When two waveforms  $f(x)$  and  $g(x)$  are not overlapping absolutely,  $C_s = 1$ .  $C_s$  is not related to a probability and only quantifies similarity of two waveforms.

### III. COMPARISON OF THE DIAGNOSTIC PERFORMANCE METRICS

In this section, the metrics reviewed in the previous section are compared in terms of four properties. Two out of the four properties are confirmed by experiments. Each diagnostic performance metric quantifies relationship between the two probability distributions, one for defect-free and another for defective. Therefore, different combinations of two normal distributions are artificially generated and values of the metrics are

TABLE I  
COMPARISON OF THE DIAGNOSTIC PERFORMANCE METRICS

	Related to test metrics	Sensitivity	Symmetric	Parametric
$FAR(w)$	Yes	High <sup>a</sup>	No	Yes
$P_{FI}(w)$	Yes	High <sup>a</sup>	Yes	Yes
$C_s$	No	Low	Yes	No
AUC	Yes	Low	Yes	No

<sup>a</sup>when  $w$  is properly set

derived for the combinations in the experiments. Afterwards, a guideline for metrics selection is proposed.

#### A. Comparison of the Metrics in Terms of Four Properties

Comparison of the four metrics using the following four properties are shown in Table I. *Relation to test metrics* such as Eq. 1 to 4 is important when you have to decide whether a value of a performance metric is enough or not. Among the metrics,  $C_s$  evaluates similarity of two waveforms and is not related to any test metrics, while the other three are inherently related to test metrics.

*Sensitivity* of the metrics is defined as slope of graphs in Figs. 7, 9, 11, i.e.  $dy/d\beta$  where  $y$  is one of the metrics and  $\beta$  is relative mean difference which is defined in the next subsection. For the visualization purpose by such graphs, sensitivity should be greater than 0.1 in the interval  $\beta$  is 2 to 3. Sensitivities in Table I are marked ‘‘High’’ when the condition is fulfilled in the experiments in the next subsection.

A diagnostic performance metric is called *symmetric* when its value is unchanged after exchanging values of  $\sigma_1$  and  $\sigma_2$  of the two normal distributions.  $P_{FI}(w)$ ,  $C_s$  and AUC are symmetric according to their definitions. Symmetric metrics do not distinguish acceptance and rejection.

*Parametric* means ‘‘assuming normal distribution’’.  $C_s$  and AUC are non-parametric and can handle arbitrary probability density functions.

#### B. Comparison using Different Combinations of Two Normal Distributions

Normal distribution is characterized by two parameters, mean  $\mu$  and standard deviation  $\sigma$  and is denoted by  $N(\mu, \sigma)$ . The probability distribution of measured values in defect-free case is denoted by  $N(\mu_1, \sigma_1)$ , and that in defective case is denoted by  $N(\mu_2, \sigma_2)$ . To express relationship of two normal distributions, we define the ratio of the two standard deviations  $\alpha = \sigma_2/\sigma_1$  and the difference between the two means relative to the standard deviations  $\beta = (\mu_2 - \mu_1)/(\sigma_1 + \sigma_2)$ .

First, two normal distributions when  $\alpha = 1$  (i.e.  $\sigma_1 = \sigma_2$ ) are considered. They are depicted in Fig. 6 for different values of  $\beta = 0, 1, 2, 3, 4$ . When  $\beta = 0$ , two distributions are overlapped completely. The values of the four metrics derived for the five combinations of the two normal distributions are shown in Table II. The metrics as functions of  $\beta$  are plotted in Fig. 7. Because  $\beta$  should be greater than 3 for practical applications, metrics should have enough sensitivity to  $\beta$  in the

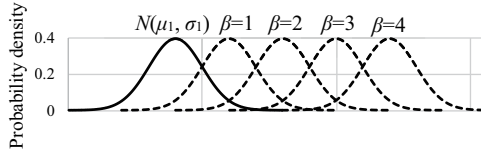


Fig. 6. Combination of two normal distributions when  $\alpha=1, \beta=1,2,3,4$  (dashed lines are  $N(\mu_2, \sigma_2)$ ).

TABLE II  
VALUES OF DIAGNOSTIC PERFORMANCE METRICS WHEN  $\alpha = 1$

$\beta$	0	1	2	3	4
FAR(5)	1.000	0.9987	0.8413	0.1587	1.350e-3
$P_{FI}(5)$	2.867e-7	1.350e-3	0.1587	0.8413	0.9987
$C_s$	0	0.6321	0.9817	0.9999	1.000
AUC	0.5	0.9214	0.9976	0.9998	0.9998

interval  $\beta$  2 to 3 to raise warning. Only two metrics FAR(5) and  $P_{FI}(5)$  fulfill the requirement.

Next, results for  $\alpha = 0.1$  and those for  $\alpha = 10$  are compared to confirm the symmetric property of the metrics. Two normal distributions when  $\alpha = 0.1$  and  $\beta = 0, 1, 2, 3, 4$  are depicted in Fig. 8. The values of the four metrics are shown in Fig. 9. Similarly, two normal distributions when  $\alpha = 10$  and  $\beta = 0, 1, 2, 3, 4$  are depicted in Fig. 10. The values of the metrics for  $\alpha = 10$  are shown in Fig. 11. Two normal distributions in Fig. 10 are the same distributions in Fig. 8 when left and right distributions are exchanged in Fig. 8. The curves of the metrics when  $\alpha = 10$  are completely the same as those when  $\alpha = 0.1$  except for FAR(5).

### C. Guideline for Selecting Diagnostic Performance Metrics

Based on the comparison result in Table I, the proposed metric selection is summarized as follows.

- When Normal distribution cannot be assumed, AUC is recommended.
- When normal distribution can be assumed,

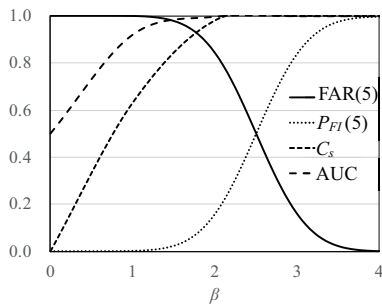


Fig. 7. Values of diagnostic performance metrics when  $\alpha = 1$ .

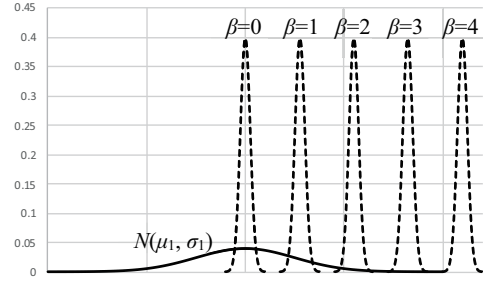


Fig. 8. Combination of two normal distributions when  $\alpha=0.1, \beta=0,1,2,3,4$  (dashed lines are  $N(\mu_2, \sigma_2)$ ).

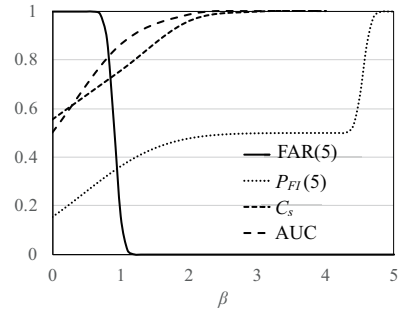


Fig. 9. Values of diagnostic performance metrics when  $\alpha = 0.1$ .

- $P_{FI}$  is recommended if both distributions are for different defective cases (i.e. defect isolation),
- FAR is recommended if two distributions are for defective and defect-free cases (i.e. defect detection).

### IV. APPLICATION TO DETECTING OPEN DEFECTS OF TSVs IN PDNs OF 3D-ICs

Generally, semiconductor circuits are fabricated on the surface of chips (or dies) in two dimensional fashion. To achieve higher integration than that of predicted by the miniaturization trend of semiconductor fabrication process, three dimensional integration is a promising approach. 3D-IC where stacked

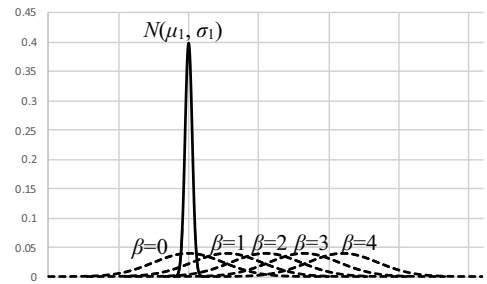


Fig. 10. Combination of two normal distributions when  $\alpha=10, \beta=0,1,2,3,4$  (dashed lines are  $N(\mu_2, \sigma_2)$ ).

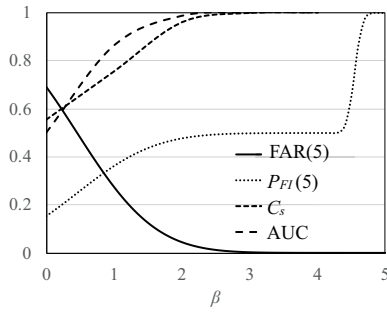


Fig. 11. Values of diagnostic performance metrics when  $\alpha = 10$ .

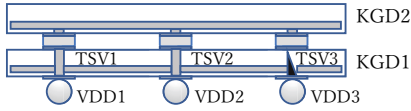


Fig. 12. Cross-sectional view of power distribution network in 3D-IC.

dies are connected by TSVs has been researched extensively so far and is adopted to applications which need high bandwidth communication between dies, such as the integration of image sensors and image processors for example [10]. In this section, the diagnostic performance metrics are applied to the test method for PDNs in 3D-ICs proposed by [11].

It is assumed that all dies in a given 3D-IC are KGDs (Known Good Dies) which have already passed die unit tests and are defect-free. The unit tests are assumed to include the test of on-chip PDN consisting of metal wires, vias and decaps, and PDNs of the KGDs have no defect. Under the assumptions, only test methods for TSVs are considered here.

Fig. 12 is a simplified cross-sectional view of PDN in 3D-IC. Two VDD distribution networks in the KGDs are connected by three TSVs under which three bumps VDD1, VDD2 and VDD3 are attached. It is assumed that the bumps are not shorted in the package and resistance between bumps can be measured at package pins. When TSV3 has an open defect, resistance between VDD2 and VDD3 will change large enough to detect from its defect-free value while resistance between VDD1 and VDD2 will be almost unchanged. Therefore the testing method is 1) locating a bump under each TSV in PDN and 2) measuring resistances between the bumps to detect open defects of TSVs.

Among the bump pairs, we want to select the best one which can avoid false acceptances and false rejections by the test as much as possible. Even though temperature of devices under test can be controlled to be constant, resistance between the selected bump pair is different from device to device due to the manufacturing process variation. The probability distribution of the resistance will change when a TSV has an open defect compared to defect-free case as shown in Fig. 2. Using one of the metrics reviewed in section II, diagnostic performances of all bump pairs are evaluated and the best one is selected to

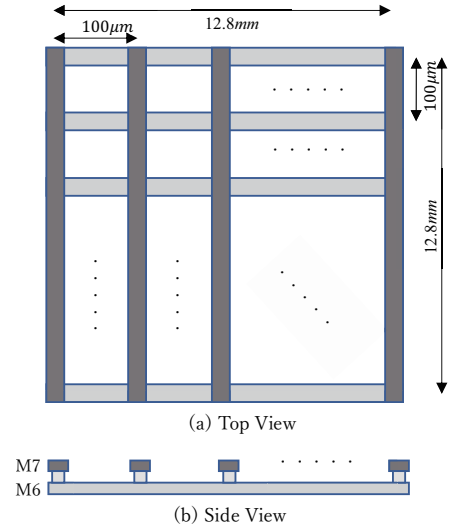


Fig. 13. Power grid dimensions.

detect the specified TSV open defect. This process is repeated for all TSVs. Although we can control trade-off between false acceptance rate and false rejection rate by changing the threshold, we have to improve the relationship between the two probability distributions to reduce the both rate simultaneously.

Experimental simulations are conducted for a 3D-IC with two dies. There are many power nets such as GND and VDD in general, only one of the nets VDD is considered here. Both two dies are 13mm square and have on-chip PDN with the regular mesh structure as shown in Fig. 13. The mesh consists of two metal layers M6 (horizontal) and M7 (vertical). Cross-sectional dimensions of the wires are the same in the two layers. The mean width  $\mu_W = 3 (\mu m)$  and relative standard deviation of the width  $\sigma_W/\mu_W = 5\%$ . The mean thickness  $\mu_T = 1 (\mu m)$  and relative standard deviation of the thickness  $\sigma_T/\mu_T = 5\%$ . Resistance of a wire segment with length  $l$ , width  $W$  and thickness  $T$  is calculated by  $R_{wire} = \rho \cdot l/(W \cdot T)$ , where  $\rho = 1.68 \times 10^{-8} (\Omega m)$  is the resistivity of Cu.  $W$  and  $T$  are constant within a layer, and are fluctuated independently with normal distribution between different layers. Resistances of vias between M6 and M7 are ignored in the experiment.

TSVs and bumps are 70 pieces each, and are placed as shown in Fig. 14. They are placed at the cross points of the power meshes in the two KGDs. Their places are described as  $\langle row number \rangle\_ \langle column number \rangle$  as 1\_13. TSVs are in cylindrical form and their mean radius  $\mu_r = 1 (\mu m)$  and relative standard deviation of the radius  $\sigma_r/\mu_r = 5\%$ . Fluctuation of their length  $l = 100 (\mu m)$  is ignored in the experiment. Resistance of a TSV is given by  $R_{TSV} = \rho \cdot l/(\pi r^2)$ , where  $\rho = 1.68 \times 10^{-8} (\Omega m)$ . Radius  $r$  is fluctuated independently for each TSV. Only open defect is considered among TSV defects and its resistance  $R_{open} = 10^{12} (\Omega)$  when open defect occurs.

Monte Carlo analysis results when TSV 1\_1 has an open defect are shown in Table III. The netlist for the circuit simulation contains 65,606 resistors and 33,281 nodes. Number of samples generated by the Monte Carlo with Latin Hyper-

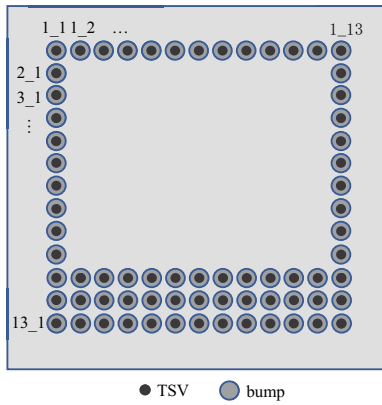


Fig. 14. Locations of TSVs and bumps.

TABLE III  
MONTE CARLO ANALYSIS RESULTS WHEN TSV 1\_1 IS OPEN

	Paired bump with 1_1				
	1_2	1_3	1_4	1_8	1_13
$\mu_1$	0.4830	0.5680	0.6245	0.7762	0.9362
$\sigma_1$	0.0191	0.0219	0.0237	0.0284	0.0336
$\mu_2$	0.6007	0.7036	0.7677	0.9279	1.0891
$\sigma_2$	0.0284	0.0323	0.0344	0.0393	0.0441
$\alpha$	1.4918	1.4742	1.4547	1.3830	1.3137
$\beta$	2.4763	2.5039	2.4649	2.2384	1.9698
FAR(5)	0.2163	0.2087	0.2351	0.4046	0.6319
$P_{FI}(5)$	0.4412	0.4556	0.4378	0.3262	0.1951
$C_s$	0.9974	0.9977	0.9973	0.9926	0.9783
AUC	0.9999	0.9999	0.9999	0.9995	0.9984

cube sampling is 3,000 to get each probability distribution. It takes 3,819.9 sec by modified spice3 run on MacBook Pro (Intel Core i5 2.7GHz, 8GB 1867MHz DDR3). The simulation is done for 12 bump pairs  $\langle 1_1, 1_2 \rangle, \langle 1_1, 1_3 \rangle, \dots, \langle 1_1, 1_{13} \rangle$ , and the results for 5 bump pairs out of the 12 pairs are shown in the table.  $\mu_1$  and  $\sigma_1$  are the mean and standard deviation of the probability distribution of defect-free case, respectively.  $\mu_2$  and  $\sigma_2$  are the mean and standard deviation of the probability distribution of defective case, respectively. The probability distributions can be assumed to be normal distributions. All four performance metrics select the bump pair  $\langle 1_1, 1_3 \rangle$  as the best one. The values of the metrics are plotted in Fig. 15. For visualization purpose, FAR(5) and  $P_{FI}(5)$  are preferable because of their higher sensitivity, while all the metrics work well for the measurement point selection.

For all other TSVs to detect their open defects,  $\alpha$  is about 1.5 and  $\beta$  is between 2 and 3 as in the above case for TSV 1\_1.

## V. CONCLUSIONS

Four diagnostic performance metrics which are proposed in literature to select measurement points for testing analog circuits are compared with respect to four properties: related to test metrics, sensitivity, symmetric and parametric. In the case study of detecting open-defects of TSVs in PDN in 3D-IC, FAR(5) and  $P_{FI}(5)$  work well to find the best bump pairs to

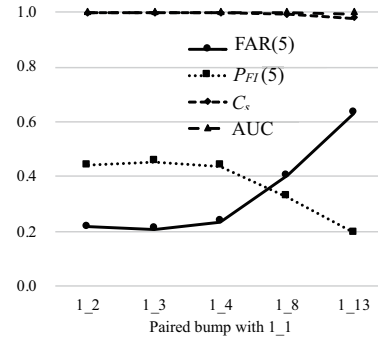


Fig. 15. Values of diagnostic performance metrics for bump pairs to detect TSV 1\_1 open defect.

measure resistance.

## ACKNOWLEDGEMENTS

The authors thank Prof. Yuhei Hatakenaka at University of Ryukyus for his introducing us ROC curve. This work was supported by JSPS KAKENHI Grant Number JP19K11883.

## REFERENCES

- [1] G. Gielen, W. Dobbelaere, R. Vanhooren, A. Coyette, B. Esen, "Design and test of analog circuits towards sub-ppm level," *2014 International Test Conference*, pp. 1-2, 2014.
- [2] K. Saab, N. Ben-Hamida, B. Kaminska, "Parametric Fault Simulation and Test Vector Generation," *Proceedings of Design, Automation and Test in Europe Conference and Exhibition 2000*, pp.650–656, 2000.
- [3] D. Zhao, Y. He, "A new test point selection method for analog circuit," *Journal of Electronic Testing*, Vol. 31, No. 1, pp.53–66, 2015.
- [4] Q. Ma, Y. He, F. Zhou, P. Song, "Test point selection method for analog circuit fault diagnosis based on similarity coefficient," *Mathematical Problems in Engineering*, Vol. 2018, p. 11, 2018.
- [5] K. Hachiya, M. Nakano, N. Himono, A. Kurokawa, Y. Hatakenaka, "TSV Open Fault Detection by Measuring Resistance between Power Pins with the Best ROC Curve", *IPSI Design Automation Symposium 2018*, pp.148–153, 2018. (in Japanese)
- [6] T. Fawcett, "An introduction to ROC analysis," *Pattern Recognition Letters*, Vol. 27, No 8, pp. 861–874, 2006.
- [7] A. K. Akebeg, "Understanding diagnostic tests 3: receiver operating characteristic curves," *Acta Paediatrica*, Vol. 96, No. 5, pp. 644–647, 2007.
- [8] Y. Hatakenaka, H. Ninomiya, E. Billstedt, E. Fernell, C. Gillberg, "ESSENCE-Q – used as a screening tool for neurodevelopmental problems in public health checkups for young children in south Japan," *Neuropsychiatric Disease and Treatment*, Vol. 13, pp. 1271–1280, 2017.
- [9] J. A. Hanley, B. J. McNeil, "The meaning and use of the area under a receiver operating characteristic (ROC) curve," *Radiology*, Vol. 143, No. 1, pp. 29-36, 1982.
- [10] D. James, "3D ICs in the real world," *25th Annual SEMI Advanced Semiconductor Manufacturing Conference (ASMC 2014)*, pp. 113-119, 2014.
- [11] K. Hachiya, A. Kurokawa, "Open defect detection of through silicon vias for structural power integrity test of 3D-ICs," *23rd IEEE Workshop on Signal and Power Integrity*, 2019.